Formation of Protein Micro-Spherulites: Thermal Aggregation of Bovine β-Lactoglobulin with Metal Ions

Jishnu Chakraborty[1], Umesh Chandra Halder[2]

Abstract— The aggregation of protein is quite relevant to the pathogenesis of several neurodegenerative diseases. Metal ion plays an accelerating role in the aggregation process. In this work, some metal ions have been chosen to study their influences on the conformation and aggregation processes of bovine β-lactoglobulin (β-lg) at equimolar ratio under thermal condition. Fe^{3+} ion causes a drastic perturbation of the conformation of native β-lg. Other metal ions, like Na^{+}, Ca^{2+}, Cu^{2+}, Zn^{2+} and Al^{3+}, merely affect the structure of β-lg except quenching of tryptophan fluorescence intensities. Fe^{3+} also influences the secondary structure of β-lg, probably by the formation of Fe^{3+}-β-lg complex which has been proposed with the spectroscopic evidences. The Cu^{2+} and Zn^{2+} ions trigger the formation of β-lg aggregates as evidenced by turbidity measurements. Formations of aggregate were identified by PAGE and SDS-PAGE studies. Thioflavin-T (Th-T) assay shows that both the Cu^{2+}-β-lg and Zn^{2+}-β-lg aggregates are fibrillar in nature. High resolution TEM images also reveal the existence of three dimensional nano- cluster with abundant nano-cavities in the Cu^{2+}-β-lg and Zn^{2+}-β-lg aggregates even at such a lower protein concentration (< 2mg mL^{-1}). The morphologic patterns, evidenced by the SEM images, reveal that Zn^{2+} form larger spherulitic oligomer/aggregates than Cu^{2+} ion at a fixed temperature. Fe^{3+} also forms small aggregates with smaller dimension than those formed by Zn^{2+} and Cu^{2+} ions. Thus it is the chemical nature of the metal ions rather than the charge factor dominates in the process of aggregation and the pattern of protein aggregates.

Index Terms— β-Lactoglobulin; Metal ions; Aggregates; Micro-spherulites, Nano-cavities.

1 Introduction

Thermal aggregation of protein is a well known phenomenon, associated with the perturbed conformation of the whole protein or of some specific domain in denatured state [1-4]. Aggregation can also be influenced by the metal ions [5-9]. These aggregates are quite relevant to pathogenesis of neurodegenerative disorders such as Alzheimer's diseases, Parkinson's diseases, and sclerosis, cardiovascular and tumoural diseases [10-12]. Primarily beta amyloidal peptide is involved in protein deposition diseases. The amyloidal plaques are predominantly composed of human β-amyloid peptide βA40, a 40-mer whose neuro-toxicity is related to its aggregation [13].

Metal ion deficiency may cause serious health hazardness in human body. Ions are being formulated with protein-based food stuffs and beverages to replenish the physical illness due to malfunctioning of enzymes, anaemia, retardation in mental development and loss of immunity in infants, children/teenagers as well as in pregnant women. As a consequence, mineral fortification strategies have been developed for the continuous/ sustainable supply of minerals through proper diet [14]. Inadequate addition of minerals thus may render severe health hazards starting from cell toxicity to organ disorder and even turns to lethal [15] while metal ion toxicity due to hyper-mineralization may also become fatal [16-17]. Survey of literature reveals that the formation and characterization of aggregates of proteins are promoted by metal ions. Several proteins, including β-lg, interact electrovalently with mono-valent ions like Na^{+}, K^{+}; di-valent metal ions like Ca^{2+}, Cu^{2+}, Zn^{2+} and tri-valent metal ions like Al^{3+} and Fe^{3+} to produce an aggregation prone conformation and accelerate the fibril formations [7, 9, 13, 18-25]. The major lacunae are the molecular level information regarding metal-protein interactions and its consequences on the patterns of the metal ion mediated protein assemblies. Thus several protein systems have been developed, having high propensity of β-amyloidal fibril formation where metal ions are found as pathogens. Hence β-lg, primarily a β-sheet protein, has been chosen as a model protein. Bovine β-lg is water soluble globular protein having 162 amino-acid residues with a molecular mass of 18,300. The crystallographic data shows that it has a predominantly β-sheet structure with nine stranded anti-parallel β-barrel and one small helix [26]. Among two tryptophans, first one (Trp19), buried in the hydrophobic core, is mainly responsible for intrinsic fluorescence properties of β-lg while the second one (Trp61) is fully solvent exposed [27].

In this article, the intrinsic fluorescence of β-lg molecule and the circular dichroic techniques have been employed to study the conformational integrity of β-lg in presence of metal ions. Moreover, efforts have been taken to understand the metal ion induced kinetic growth of aggregates turbidometrically and to study the nature of aggregates with the help of Thioflavin-T assay and electron microscopic techniques (SEM,

- [1]*Camellia Institute of Engineering & Technology, Budbud, NH2 By Pass (North), Burdwan, 713403, E-mail: jis_john1@yahoo.co.in*
- [2]*Organic Chemistry Section, Department of Chemistry, Jadavpur University, 188, Raja S. C. Mullik Road, Kolkata-700032, India, uhalder2002@yahoo.com.*

TEM).

2 Materials and Methods

2.1 Materials

Bovine β-lg was purified from fresh cow milk [28-29]. Its concentration was determined using ε_{280}=17,600 M^{-1} cm^{-1}. AR grade sodium dihydrogen phosphate and disodium hydrogen phosphate were purchased from Sisco Research Laboratory, India. AR grade NaCl, $CaCl_2$, $CuCl_2$, $ZnCl_2$, $AlCl_3$, $FeCl_3$, hydrochloric acid, ammonia, methanol, acetic acid, glycerol etc. were obtained from Merck, India. Acryl amide, bis- acryl amide, N, N, N, N′-tetramethylethylenediamine (TEMED), ammonium persulphate, SDS, bromophenol blue, coomassie blue, Tris buffer, 8-amino-1-napthalenesulphonic acid (ANS) were purchased from Sigma Chemical Co., U.S.A.

2.2 Fluorescence measurements

Fluorescence measurements of β-lg solutions containing metal ions were performed using the Spex Fluorolog II (USA) spectrofluorometer with an excitation wave length of 295 nm and emission wavelength in the range of 310-550 nm according to the method of J. C. Allen and S. Jeyarajah [30]. Here protein to metal ratio was maintained at 1:1 in molar proportion and spectra were compared with the native one. All data points were an average of triplicate measurements and correspondingly blank corrected.

2.3 Circular dichroic measurements

Far UV-CD experiments were carried out with a JASCO J-815 spectropolarimeter at 25° C where different metal ions were added to native β-lg solutions using a cylindrical cell of path length 1mm. Solutions were made in 10 mM sodium phosphate buffer, pH 6.5. All the β-lg solutions, having concentrations 2mg ml^{-1} (1mM) and containing equimolar metal ions, were used for far UV-CD spectra measurements. Typical instrumental parameters used were: path length=1.0 mm, sensitivity=50 m deg (for far UV), time constant 2 s, step resolution = 0.2 nm/data and scan speed 20 nm/min. Far UV range scanned was 200-250 nm. Each spectrum was the average of three consecutive scans subtracted from the corresponding blank. The smooth spectral profiles were achieved using the polynomial curve-fitting program.

2.4 Turbidity measurements

Turbidity studies of the solutions of native β-lg containing metal ions (1:1) were performed in a JASCO V-670 spectrophophotometer (Jasco, Japan) attached with a Peltier thermostat temperature controller (model EHC-716) along with the Spectra Manager software. A quartz cuvette of 1 cm path length was used and optical densities were measured at 400nm. Experiments were done in two steps. Firstly, optical densities (OD_{400nm}) for all experimental solutions were measured at 10 °C intervals within the temperature range of 25-80°C and in the second step, turbidities appeared due to formation of protein aggregates were measured with the time duration of 1hour at a constant temperature (70 °C) at 10 minute time intervals.

2.5 Detection of Aggregates by native and SDS-PAGE

Both native and SDS-PAGE were carried out using 15% acryl amide resolving gel [31]. Aliquots (20μL) of heat treated β-lg solutions containing metal ions were loaded in the wells. Gels were stained with Coomassie Brilliant Blue R 250. A molecular weight marker ranging from 10-170 kDa (PageRuler™, Prestained Protein Ladder, Fermentus Life Science, UK) was ran in parallel with the SDS-PAGE to determine the molecular weights of the β-lg aggregates.

2.6 Identification of fibrillar aggregates by Thioflavin-T (Th-T) assay

Th-T binding assay was performed using a Spex Fluorolog II (USA) spectrofluorometer with an excitation wave length of 440 nm and the emission was monitored at 490 nm. The aliquots of 0.1ml of heat treated (70 °C) β-lg solutions were transferred into 2.5 ml of phosphate buffer (pH 6.8) and after 1 hour ultra-sonication the samples were treaded with 10μL of Th-T solution. The final concentration of Th-T was 50μM and the spectra were recorded at 25°C. All the spectra were an average of triplicate measurements and blanks were corrected.

2.7 Studies of the morphology of the oligomer/aggregates

Characterizations of oligomer/aggregates of β-lg were performed with the Scanning Electron Microscope (SEM, model no. JEOL JSM-5200, Tokyo, Japan) within 0.5-30 kV range on a glass substrate. Aliquots of heat treated β-lg solution containing metal ions were spread over the glass slides and left for air drying at room temperature. This process was repeated for twice to achieve a detectable amount of oligomer/aggregates and finally gold coated before scanning under the electron microscope.

2.8 Transmission electronmicroscopy

Copper grids were prepared by negative staining immediately the preparation of the samples for transmission electron microscopy. The sample solutions were sonicated for ~60 sec and diluted 50-150 times. A droplet of the diluted sample was put onto a carbon support film on a copper grid of 300 square meshes. After 20 sec the droplet was removed with a filter paper followed by a droplet of 2% uranyl acetate (Sigma, Steinheim, Germany) solution was put on the grid and finally removed after 15 sec and left for air-dry. The micrographs were then taken by using high-resolution transmission electron microscope (JEOL-TEM-2011, Tokyo, Japan) with an accelerating voltage of 80-85 kV in different magnification.

3 Results and Discussions

3.1 Fluorescence of β-lg in presence of metal ions

Effect of metal ions on the tertiary structure of native β-lg was monitored by intrinsic fluorescence measurements. Fluorescence emission spectral patterns of tryptophans of β-lg in presence of mono (Na^+, K^+), di (Ca^{2+}, Cu^{2+}, Zn^{2+}) and tri-valent (Al^{3+}, Fe^{3+}) metal ions have been represented in Fig. 1A. The tertiary structure of β-lg was mostly influenced by the Fe^{3+} and Cu^{2+} ions at equimolar metal-protein concentrations (Fig.

1A).

Quenching of Trp fluorescence intensity was observed in presence of bi-valent Cu^{2+} ion without any significant shift in emission maxima. Other mono-valent and di-valent metals like Ca^{2+} and Zn^{2+} did not exhibit any impact on the tertiary structure of β-lg apart from mild alteration in fluorescence intensities. The most important observations were obtained with Cu^{2+} and Fe^{3+} ions which are also paramagnetic in nature and induce the quenching of fluorescence intensities of tryptophan in β-lg. This quenching is probably due to either direct collision or by complex formation [32]. Interestingly, Fe^{3+} induced drastic quenching of fluorescence intensity accompanying with the red shift in emission maxima (333nm to 350nm) implies a strong indication of tertiary structural perturbation of β-lg. Concomitant addition of Fe^{3+} ion clearly indicates the structural distortion surrounding the micro-environment of Trp19 (Fig. 1B). Although Fe^{3+} ion shows broad absorption spectrum within the excitation (295 nm) and emission (330-350 nm) region of tryptophan in free state as well as in β-lg (inset, Fig. 1B). The fluorescence quenching accompanied by red shift in β-lg is more pronounced rather than the quenching of free tryptophan in aqueous solution (data not shown), indicating the conformational distortion by complex formation. Similar quenching behavior has also been reported earlier by Xu et al., 2008, without any shift in emission maxima in case of BSA [32].

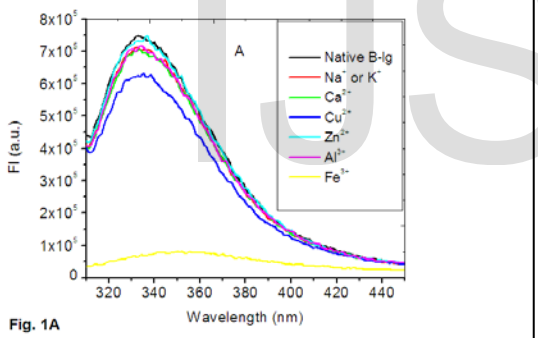

Fig. 1A

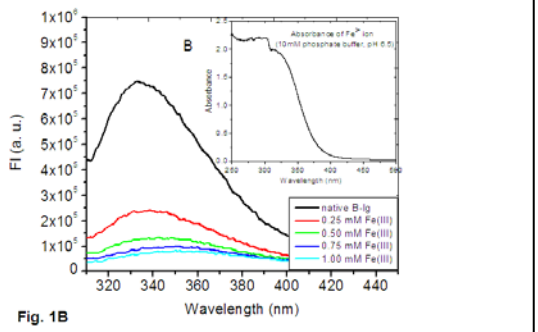

Fig. 1B

Fig. 1. (A) Intrinsic fluorescence emission spectra of β-lg (1mM) in presence of metal ion at equimolar (1:1) concentration. Excitation wavelength was set at 295 nm and emission was recorded within the range of 310 nm to 450 nm. Solutions were prepared in phosphate buffer (10 mM, pH 6.5) and spectra were recorded at room temperature.

Fig. 1. (B) Intrinsic fluorescence emission spectra of β-lg in presence of varying Fe^{3+} metal ion concentrations. Here the black line represents the native β-lg, red (0.25 mM), green (0.5 mM), blue (0.75 mM) and cyan (1.0 mM) of Fe^{3+} ion respectively at a fixed concentration of β-lg (1 mM) at identical condition. The UV absorption spectra of 0.5mM Fe^{3+} ion in 10 mM phosphate buffer, pH 6.5 shows its absorbance within the entire excitation and emission range of tryptophan (Inset). All the data points were an average of three consecutive measurements and correspondingly blank corrected.

The tri-valent Al^{3+} ion could not affect the intrinsic fluorescence of β-lg. Copper and iron possibly try to ensure their coordinations in the β-lg environment. Consequently quenching of intrinsic fluorescence intensities is thus observed [33].

3.2 UV CD of β-lg in presence of metal ions

Influences of bi-valent metal ions on the far-UV CD spectrum of native β-lg were relatively consistent. Only changes in ellipticity values in the wavelength region of 208-210 nm were observed in case of Cu^{2+} (Fig. 2A). This was probably due to the bindings of Cu^{2+} to β-lg in native state and consequently the alteration in local conformation of β-lg took place. Thiol (Cys121) mediated copper bridged dimer formation of β-lg has been reported earlier where reactivity of buried –SH group increases at the expense of small α-helix [8]. Nonetheless binding probability through His146 and His161 of β-lg has also been proposed by other authors [6], with a similar destabilization of structure of β_2-microglobulin [34-35]. Similar observations have been reported with other proteins like α-synuclein, involved in Parkinson's diseases and in prion protein in Cretzfeld-Jacob diseases [36-37]. Indeed, the differences observed with the effect of other mono- and di-valent metal ions seem to be in the noise, may be Cu^{2+} binding to the protein induces a weak charge transfer which affect the UV-region. The other bi-valent metals failed to perturb the native global conformation of β-lg.

The catastrophic effect brought down into the structure of native β-lg when tri-valent Fe^{3+} comes to play (Fig. 2B). The characteristic β-sheet signal (215-216 nm) disappeared with the increase in the random coil structure and thus loosing the gross structural integrity. This was probably due to formation of new species (Fe- β-lg complex). The $FeCl_3$ promoted partial and irreversible conformational changes of β-lg A, with a combined effect of heat and acidification (pH 1.5-3), were observed without any considerable denaturation of protein molecule [9]. In our case, there was a drastic loss of conformational integrity where pH of the solution was above isoelectric point (5.1 for β-lg) and maintained nearly at 6.5. Some of the side chains residues exist as negatively charged species (e.g. aspertate, glutamate) at this pH. Nonetheless, from the crystallographic structures of β-lg, it can be proposed that the aromatic side chains from the four tyrosine residues (Tyr20, Tyr42, Tyr99 and Tyr102) and two tryptophan residues (Trp19 and Trp61) are very much susceptible to complex formation with Fe^{3+} ions at this physiological pH by cation-π type interaction. This interaction can be evidenced by the changes in signal of the aromatic moieties in the near-UV CD region (Fig. 2C). Moreover, at extreme acidic condition, the free –SH group remains buried into the hydrophobic patch of β-lg and remains inert. Higher the pH value, the higher is the reactivity of –SH group and its accessibility to solvent/metal ions. Charge factors on surface and in the core are less significant in

the context of global structural stabilization of β-lg, because in presence of Al^{3+} β-lg was able to sustain its secondary structural integrity. Nonetheless, similar stability of β-sheet structure was observed even at higher concentration of monovalent Na^{+} ions which remain simply as an electrolyte (data not shown).

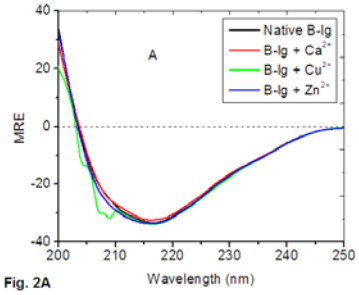

Fig. 2A

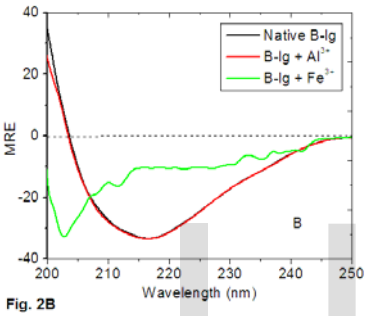

Fig. 2B

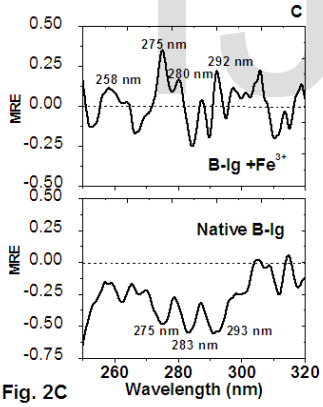

Fig. 2C

Fig. 2. (A) Far UV- CD spectral pattern of native β-lg (black line) in presence of equimolar (1:1) bi-valent Ca^{2+} (Red), Cu^{2+} (green) and Zn^{2+} (blue) metal ions respectively. Solutions were prepared in phosphate buffer (10mM, pH 6.5) and spectra were recorded within the wavelength range of 200 nm to 250 nm at room temperature.

Fig. 2. (B) Far UV- CD spectral pattern of native β-lg (black line) in presence of equimolar (1:1) tri-valent Al^{3+} (Red) and Fe^{3+} (green) metal ions respectively. Solutions were prepared in phosphate buffer (10mM, pH 6.5) and spectra were recorded within the range of 190 nm to 250 nm at room temperature.

Fig. 2. (C) Near UV-CD spectral pattern of native β-lg (lower panel) and β-lg + Fe^{3+} (upper panel) at 1:1 molar ratio in 10 mM phosphate buffer, pH 6.5. Spectra were recorded within the range of 250 nm to 320 nm at room temperature. All the data points were an average of three consecutive scans and correspondingly blank corrected.

3.3 Turbidities of β-lg in presence of metal ions

Appearance of turbidity, as measured with the OD_{400nm} of only β-lg aggregates, was observed after reaching the temperature 80 °C (Fig. 3A).

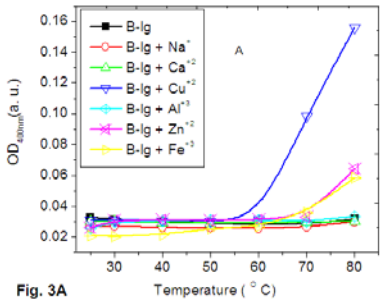

Fig. 3A

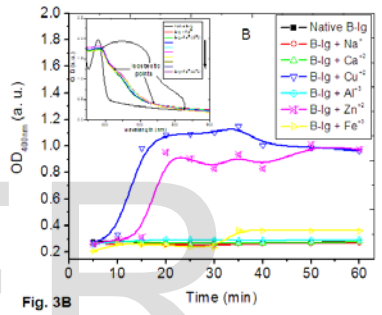

Fig. 3B

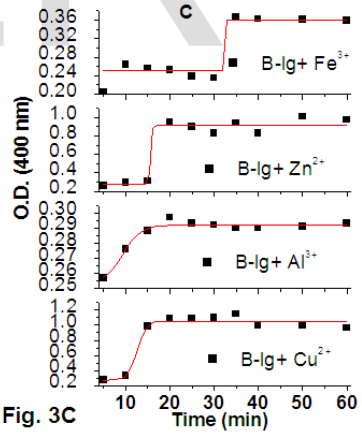

Fig. 3C

Fig. 3. (A) Temperature-dependent and (B) Time-dependent turbidity profiles of β-lg in presence of metal ions at equimolar (1:1) concentrations. Optical density was measured at 400nm after 10-15 min incubation of the sample solutions after reaching the exact temperature. Optical path length of the quartz cuvette was 1cm. In case of time dependent study, data recorded at 10 min time interval during 1hour at fixed temperature (70 °C). Here the lines correspond as follows: Native β-lg (black), β-lg + Na^{+} (red), β-lg + Ca^{2+} (green), β-lg + Cu^{2+} (blue), β-lg + Al^{3+} (cyan), β-lg + Zn^{2+} (pink), β-lg + Fe^{3+} (yellow) metal ions respectively. Appearance of the isosbestic points in β-lg + Fe^{3+} spectral pattern indicates the complex formation (3B, Inset). (C) Turbidity with a sigmoid fitting curve as a function of time (upto 1 hour at a 10 min time interval) have been presented in case of β-lg in presence of Cu^{2+}, Al^{3+}, Zn^{2+} and Fe^{3+} ions at 1:1 molar ratio in 10 mM phosphate buffer, pH 6.5. Best fitted sigmoid curves were obtained only for these four ions. Data points were an average of triplicate measurements.

Sudden rise in optical density of β-lg solution in presence of Cu^{2+} ion was experienced during elevation of temperature immediately after 60-65 °C, whereas the effects of Zn^{2+} and Fe^{3+} were relatively less than that of Cu^{2+} ion at 1:1 molar ratio. Indeed Cu^{2+} is known to precipitate in phosphate buffer and consequently a control experiment was also performed and values were deducted from the sample solution. Changes in optical densities were found more prominent in case of bi-valent Cu^{2+} followed by Zn^{2+} and tri-valent Fe^{3+} compared to native β-lg without any metal ions. Moreover the mono-valent metal ions like Na^{+} or K^{+}, bi-valent Ca^{2+} and trivalent Al^{3+} ions fail to trigger the β-lg aggregation at this molar ratio. High molecular aggregates are formed in presence of Ca^{2+} ion only when calcium to protein ratio remains above 10:1 molar [7].

With the evolution of time, upto 1 hour at pre-aggregation condition (70 °C), the appearance of turbidities of β-lg solution were significant in presence of Cu^{2+} and Zn^{2+} ions (Fig. 3B). No further appearance of turbidity was noticeable in presence of Fe^{3+} ion even after 30 minutes apart from preliminary rise in optical density. Increase in OD values at 400nm was at the cost of formation of new species with the interaction of β-lg in native state (Fig. 3B, Inset). Role of Al^{3+} ion was less significant at this molar ratio (1:1). Though the turbidity value reaches maxima within a very short period of time, but no further increase in optical density in presence of Al^{3+} ion was achieved. Turbidity as a function of time at a fixed temperature (70°C) was fitted with sigmoid curve. Best fitting curves were obtained with four metal ions like Cu^{2+}, Al^{3+}, Zn^{2+}, Fe^{3+} (Fig. 3C). In brief, the progress of aggregates formation was triggered by the Cu^{2+} ions with the temperature elevation and incubation time, followed by Zn^{2+} and Fe^{3+} ions. But Ca^{2+} and Al^{3+} have no significant effect at this molar ratio. Mono-valent Na^{+} and K^{+} act as simple co-electrolytes in the aqueous solution of β-lg.).

3.4 Polyacrylamide (PAGE) and Sodium dodecyl sulfate-polyacrylamide (SDS-PAGE) results

The native and SDS-PAGE (Fig. 4A and Fig. 4B respectively) patterns illustrate that the forces involved in the formation of aggregates are either of co-valent type or non-covalent (ionic/ hydrophobic). At lane 1 (β-lg+Fe^{3+}), bands appeared in high molecular weight range along with the monomer band. It signifies the formation of co-valently linked large molecular aggregates which fail to penetrate the resolving gel. In lane 2 (β-lg+Zn^{2+}), several bands were appeared in both the native and SDS-PAGE along with the monomer band which signifies the presence of aggregates/ oligomer of different molecular weights. All these aggregates and oligomers are covalently linked as evidenced by their appearance in SDS-PAGE.

At lane 3 (β-lg+Al^{3+}), the dimeric band appeared at slightly higher in position in native PAGE which finally vanishes in SDS-PAGE and a smearing occurs from the high molecular weight range. The exact reason of disappearance of monomer/ dimer band in SDS-PAGE is not clear but in presence of SDS, the sulphonate groups probably interact with Al^{3+} ion bound to β-lg, so that coagulation of β-lg takes place. It was evident that relative mobility of the dimer band in native gel was less compared to other lanes due to alteration of surface charges.

In lane 4 (β-lg+Cu^{2+}), dimer band appeared in native gel and the same dimer band became more prominent in SDS-PAGE pattern. This signifies that Cu^{2+} ion mediated monomer to dimer conversion is more effective under denaturing condition. Primarily, the effect of heat makes β-lg more prone to be conformationally distorted and secondly, SDS triggers permanent structural disorder that helps Cu^{2+} ion to facilitate free –SH oxidation during disulfide linked dimer formation [8, 38].

In lane 5 (β-lg+Na^{+}) and lane 6 (β-lg+Ca^{2+}) no significant bands corresponding to large molecular aggregates were found except less intense dimer fraction as observed in case of native β-lg (lane 7, native PAGE). Large molecular aggregate formations are not possible with Na^{+} and Ca^{2+} ions at this concentration. All the bands appeared in the SDS-PAGE were compared with the pre-stained marker of known molecular weight (lane 7, SDS PAGE).

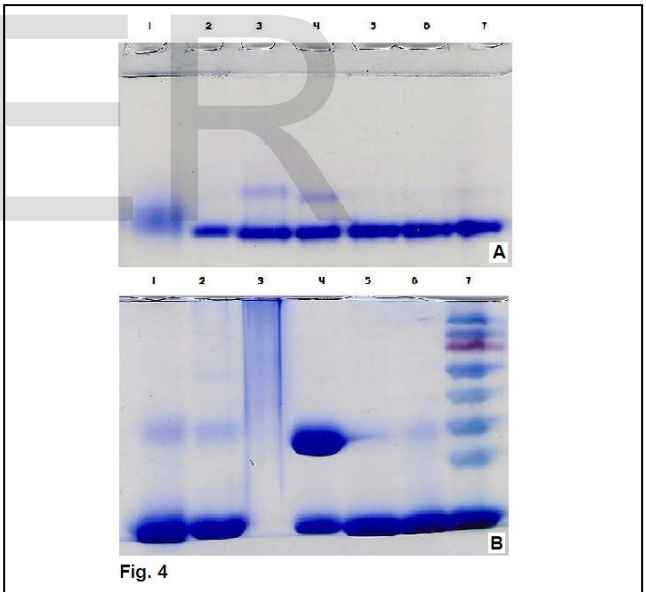

Fig. 4

Fig. 4. (A) Native PAGE pattern and (B) SDS-PAGE pattern of heat treated β-lg in presence of metal ions. Lens correspond to as follows: β-lg + Fe^{3+} (lane 1), β-lg + Zn^{2+} (lane 2), β-lg + Al^{3+} (lane 3), β-lg + Cu^{2+} (lane 4), β-lg + Na^{+} (lane 5), β-lg + Ca^{2+} (lane 6) and β-lg (native) along with pre-stained protein ladder ranging from 10-170 kDa (PageRuler™, Prestained Protein Ladder, Fermentus Life Science). Protein and metal ratio was maintained 1:1 in all the cases during heat treatment.

3.5 Fibril specific Th-T assay

Thioflavin-T (Th-T) is known to specifically bind rapidly to amyloid fibrils accompanied by dramatic increase in fluorescence intensity within the range of 450 – 550 nm upon excitation at 440nm [39]. This fibril specific probe shows significant rise in fluorescence with heat treated β-lg solutions [6].

ions (Fig. 6 c-d). The Zn^{2+} ion induced large aggregate formation of β-lg has been evidenced by Navarra et al, 2007 by dynamic light scattering measurements earlier [5].

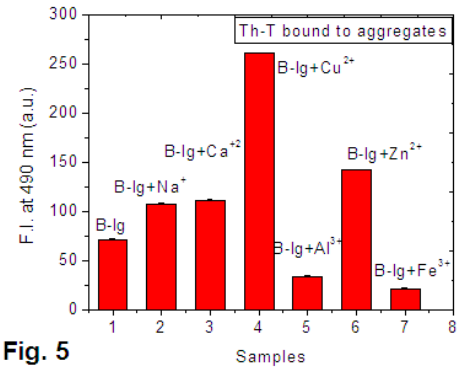

Fig. 5. Thioflavin T binding to the fibrillar aggregates of β-lg in presence of metal ions. Excitation wave length was selected at 440 nm and emission maxima for all sample solutions were monitored at 490 nm in phosphate buffer (pH 6.8). Final concentration of Th-T was 50μM and spectra were recorded in triplicate at 25 ˚C. All the spectra were deducted from the corresponding blanks and presented as an average of triplicate measurements. Percent errors were represented in terms of error bars in the corresponding bar diagrams.

Fluorescence intensity of Thioflavin-T at 490nm was maximum in case of β-lg+Cu^{2+} complex followed by β-lg+Zn^{2+} complex, indicating the formation of β-amyloids or fibrillar aggregates/oligomer (Fig. 5). Fluorescence intensities are highly quenched in case of Al^{3+} and Fe^{3+} ions. Nonetheless transition metal ions are significant fluorescence quenchers [40]. It may appear to be inconclusive whether iron induced aggregates are fibrillar or non-fibrillar at present but undoubtedly it can be said that copper- β-lg and zinc- β-lg aggregates are fibrillar in nature. The β-lg+Ca^{2+} and β-lg+Na^{+} complexes also show a little enhanced fluorescence intensities, the charge distribution ratio might be the reason. High molecular aggregates are formed in presence of Ca^{2+} ion only when calcium to protein ratio remains above 10:1 molar [7].

3.6 Morphology of oligomer/ aggregates

The morphologic patterns of metal ions (particularly Cu^{2+}, Zn^{2+} and Fe^{3+}) induced aggregates are presented in the Fig. 6 (a-f). It is clearly seen that the Zn^{2+} ion mediated aggregates are spherulitic in pattern with larger dimensions (10-40 μm) compared to Cu^{2+} ions and the pattern of the Cu-aggregates are not distinctly sphere like Zn^{2+}. The clustered and/or agglomerated distributions are visible under scanning of Cu^{2+} mediated aggregates (Fig. 6, a-b). The fractures in the spheres are probably due to the shrinking of the spherulites because of dehydration under vacuum. The surface of the large spherulites was imaged with higher magnifications near the cracks which is composed of small spherulitic aggregates (< 1μm), with the manifestation of a rough surface in presence of Zn^{2+}

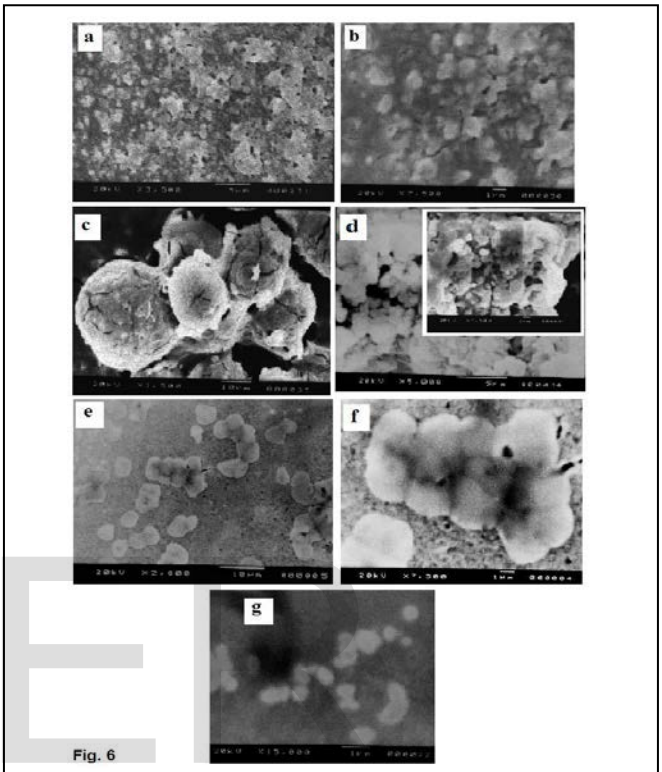

Fig. 6. Scanning electron micrographs of heat treated β-lg aggregates in presence of Cu^{2+} ion (a-b), Zn^{2+} ion (c-d) and Fe^{3+} ion (e-f). SEM image of only β-lg without any metal ions has been also presented as a control (Fig. 6 g). β-lg (2mg mL^{-1}) solutions containing metal ions (1:1) were heat treated at 70˚C for 1hour in phosphate buffered solution (10 mM, pH 6.5) and spread over glass substrates. Sample stubs were air dried and coated with gold and scanned under electron microscope. The scale bar of the micrographs is within 1-10 μm (inset of Fig. 6b: 1um).

Characterization of this aggregates under microscopic scale bar made it possible to understand that the aggregation process is merely affected by the charge of the metal ions rather than the nature of the ions regulating the size and dimensions of the aggregates.

This becomes more prominent when the distribution patterns of β-lg aggregates in presence of Fe^{3+} ion were imaged under SEM. Nicely formed sphere like aggregates were mutually associated and distributed ranging from 1μm to 20 μm (Fig. 6, e-f). The microstructures of native β-lg consists of a rather monodisperse spherulites with size of 50-100 nm up to few microns, depending on the thermal history and concentrations [41]. Microscopic image of only β-lg aggregates were also presented without any metal ions as control (Fig. 6, g). Therefore it can be assumed that the spherulitic forms of the aggregates might be the fundamental unit in aggregation processes but the nature of their agglomeration is strictly regu-

lated by the nature of metal ions. The charge factor here becomes less significant whereas the chemical nature of the metal ions dominates the agglomeration process and pattern formation. Thus electron microscopic images provide the morphology of the aggregates formed with different metal ions regarding their shape/size and dimensions.

3.7 TEM results

Preliminary evidence for the formation of fibrillar aggregate was obtained from Th-T assay and the role of Cu^{2+} and Zn^{2+} were significant in the formation of such aggregates. The investigations under high-resolution TEM images (Fig. 7a and 7b) reveal the existence of three dimensional nano-fibrillar cluster networks with abundant nano-cavities in the range of 50-100 nm. Particularly the fibril formation of β-lg is common bio-physical process at higher concentrations [42-44]. Here compact network formation at such a lower concentrations (~2mg ml^{-1}) is undoubtedly an alarming situation for amyloidal pathogenesis. On the basis of the results obtained in SDS-PAGE studies we were also interested with β-lg-Fe^{3+} aggregates. But it failed to response the Th-T assay. It became clear that the process of aggregation was different from the previous cases due to alteration in β-sheet conformation of the native protein.

The TEM images obtained under different resolutions and dimensions shows that the nature of aggregates of Fe+β-lg was mostly complex-cluster type along with the partly fibrillar form (Fig. 7c). Overlapping of clusters was also present even after sonication followed by dilution and fixation to TEM grids. A cloudy layered pattern appeared but large aggregates were distinctly detectable, probably due to the complex formation with iron. Apparently the SEM images are likely to be similar in nature with spherulitic pattern of different microscopic dimensions but the internal structure of the aggregates differs depending on the nature and reactivity of the metal ions irrespective of their charges.

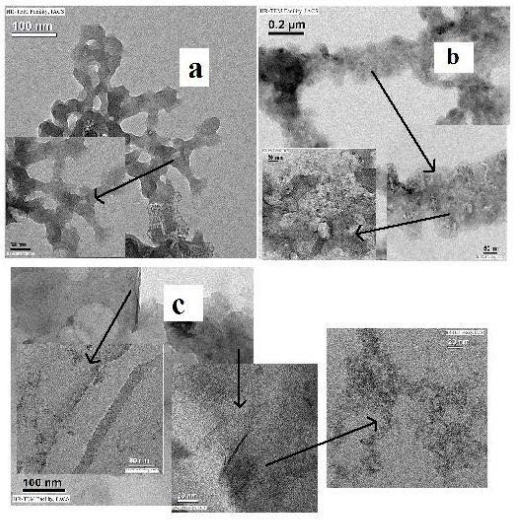

Fig. 7

Fig 7. Transmission electron micrographs of heat treated (a) Cu+β-lg aggregates (scale bar: 100 nm and 50 nm for inset), (b) Zn+β-lg aggregates (scale bar: 0.2 µm; 50 nm and 20 nm for inset) and (c) Fe+ β-lg aggregates (scale bar: 100nm; 50nm and 20 nm for insets) at 70°C for 1hr in phosphate buffer solution (10 mM, pH 6.5). High resolution TEM images obtained after ~ 60 sec sonication of sample solutions followed by 50-150 times dilution

4 Conclusion

Together with the results obtained and discussed, it is evident that some metal ion like Fe^{3+} affects both the secondary and tertiary structure of native β-lg at pH 6.5. The significant changes in structure were probably due to the formation of Fe-β-lg complex. Other metal ions like, Na^{+}, Ca^{2+}, Cu^{2+}, Zn^{2+} and Al^{3+}, do not influence the structure of native β-lg except the quenching of fluorescence intensities. Metal ions like Zn^{2+} and Cu^{2+} directly participate in the process aggregation of β-lg. The thermal perturbation makes β-lg prone to form irreversible aggregates by inter-protein cross-linking and/or metal-complex formation. Though both the metals favor the aggregation of β-lg with temperature elevation and time evolution, the aggregation kinetics were different. The β-lg -Cu^{2+} interaction is specific and binding with the protein in the native state is favored. This binding changes the local conformation of β-lg (changes observed in far-UV CD spectrum of β-lg with Cu^{2+} ion). Thiol (Cys121) mediated copper bridged dimer formation of β-lg has also been reported earlier, moreover binding possibilities of Cu^{2+} through His146 and His161 of β-lg have also been proposed. Nonetheless Cu^{2+} metal ion is more effective than Zn^{2+} or Fe^{3+} (sudden rise in optical density value at 400 nm occurs during turbidity measurements in case of Cu^{2+} ion after 60-65°C). Thus it is clear that Cu^{2+} ion will be more dangerous than Zn^{2+} metal ion, causing faster aggregates in vitro. Both the β-lg aggregates with Cu^{2+} and Zn^{2+} are fibrillar in nature while the higher molecular aggregates with Fe^{3+} ion are of different type. From the studies of morphologies of the oligomer/ aggregates in the SEM studies, it is evident that Zn^{2+} ion mediated β-lg aggregates are spherulitic in pattern with larger dimension (10-40 µm) compared to Cu^{2+} metal ion mediated aggregates. The Cu^{2+}-β-lg aggregates are not completely sphere-like. The high resolution TEM images showed the existence of three dimensional nano-fibrillar cluster networks with plenty of nano-cavities in the range of 50-100 nm. The differences in the TEM images were likely to be due to difference in the mechanistic pathway of protein-protein/ protein-metal complex formation. Therefore the kinetic growth and the shape of the β-lg aggregates with different metal solely depend on the nature of the metal ions, not on the charge of the metal ions.

Acknowledgment

Financial support of UGC-CAS (Govt. of INDIA), Department of Chemistry, Jadavpur University, Kolkata is gratefully acknowledged. Authors also like to acknowledge University Scientific Instrumentation Centre (U. S. I. C.) of Jadavpur University, Kolkata and Indian Association for the Cultivation of Science (I. A. C. S.), Kolkata, for providing electron microscopic instrumental facilities. Authors also like to acknowledge Camellia Institute of Engineering & Technology, Budbud, Burdwan, WB, India, for providing academic and administrative help.

REFERENCES

[1] W.L. Chen, M. T. Huang, C. Y. Liau, J. C. Ho, K. C. Hong, S. J. T. Mao, "β-lactoglobulin is a thermal marker in processed milk as studied by electrophoresis and circular dichroism spectra", *J. Dairy Sci.,* vol. 88, pp1618-1630, 2005.

[2] H. H. J. de Jongh, T. Groneveld and J. de Groot, "Mild isolation procedure discloses new protein structural properties of β-lactoglobulin", *J. Dairy Sci.,* 84, pp 562-571, 2001.

[3] V. Militello, V. Vetri, M. Leone, "Conformational changes involved in thermal aggregation process of bovine serum albumin", *Biophys. Chem.,* 105, pp 133-141, 2003.

[4] V. Vetri, V. Millitelo, "Thermal induced conformational changes involved in the aggregation pathways of beta-lactoglobulin", *Biophys. Chem.,* 113, pp 83-91, 2005.

[5] G. Navarra, M. Leone, V. Militello, "Thermal aggregation of β-lactoglobulin in presence of metal ions", *Biophys. Chem.,* 131, pp 52-61. 2007.

[6] Stripe, B. Rizzuti, M. Pantusa, R. Bartucci, L. Sportelli, R. Guzzi, "Thermally induced denaturation and aggregation of BLG-A: effect of the Cu^{2+} and Zn^{2+} metal ions", *Eur. Biophys. J.,* 37, pp 1351-1360, 2008.

[7] J. W. F. A. Simons, H. A. Koster, R. W. Visschers, H. H. J. de Jongh, "Role of calcium as trigger in thermal β-lactoglobulin aggregation", *Arc. Biochem. Biophys.,* 406, pp 143-152, 2002.

[8] S. Bouhallab, G. Henry, F. Caussin, T. Croguennec, J. Fauquant, D. Molle, "Copper-catalyzed formation of disulfide-linked dimmer of bovine β-lactoglobulin", *Lait,* 84, pp 517-525. 2004.

[9] K. Watanabe, K. Nobuo, t. Matsuda, R. Nakamura, "Effect of iron (3+) chloride on heat denaturation of beta–lactoglobulin A in acid media", *J. Agric. Food Chem.,* 33, pp 403-405, 1985.

[10] Ross, M. A. Poirier, "Protein aggregation and neurodegenerative disease", *Nat. Med.,* 10:S10-S17. doi: 10:1038/nm1066, 2004.

[11] S. Frokjaer, D. E. Otzen, "Protein rug stability-a formulation challenge", *Nat. Rev. Drug Disco.,* 4, pp 298-306, 2005.

[12] J. S Pedersen, D. E. Otzen, "Amyloid - a state in many guises: Survival of the fittest fibril fold", *Prot. Sci.,* 17, pp 2-10, 2007.

[13] P. W. Manyth, J. R. Ghilardi, S. Rogers, E. De Master, C. J. Allen, E. R. Stimson, "Aluminium, iron and zinc ions promote aggregation of physiological concentrations of β-amyloid peptide", *J Neurochem.,* 61, pp 1171-1174, 1993.

[14] J. E. O'Connell, P. F. Fox, "Effect of beta-lactoglobulin and precipitation of calcium phosphate on the thermal coagulation of milk", *J. Dairy Res.,* 68, pp 81-94, 2001.

[15] S. Morante, R. GonzaLez-Iglesias, C. Ptrich, C. Meneghini, W. Meyer-Klaucke, G. Menestrina, M. Gasset, "Inter- and Intra- octarepeat Cu(II) site geometries in the prion protein: implications in Cu (II) binding cooperativity and Cu(II)- mediated assemblies", *J. Biol. Chem.,* 279, pp 11753-11759, 2004.

[16] C. D. Syme, R. C. Nadal, S. E. Rigby, J. H. Viles, "Copper binding to the amyloid-β (Ab) peptide associated with Alzheimer's disease: folding, coordination geometry, pH dependence, stoichiometry, and affinity of Aβ-(1-28): insights from a rage of complementary spectroscopic techniques", *J. Biol. Chem.,* 279, pp 18169-18177, 2004.

[17] Y. Mekmouch, Y. Coppel, K. Hochgrafe, L. Guilloreau, C. Talmard, H. Mazarguli, P. Faller, "Characterisation of the ZnII binding to the peptide amyloid β-1-16 linked to Alzheimer's diseases", *Chem. Biochem.,* 6, pp 1663-1671, 2005.

[18] S. Zirah, S. A. Kozin, A. K. Mazur, A. Blond, M. Cheminant, I. Segalas-Milazzo,P. Debey, S Rebuffat, "Structural changes of region 1-16 of the Alzheimer disease amyloid beta-peptide upon zinc binding in vitro aging", *J. Biol. Chem.,* 281, pp 2151-2161, 2006.

[19] R. C. McLachlan, A. J. Dalton, T. P. A. Kruck, B. Y. Bell, W. L. Smith, W. Kalow, D. F. Andrews, "Intramuscular desferrioxamine in patients with Alzheimer's diseases", *Lancet,* 337, pp 1304-1308, 1991.

[20] K. Suzuki, T. Miura, H. Takeuchi, "Inhibitory effect of copper (II) or zinc (II)- induced aggregation of amyloid β-peptide", *Biochem. Biophys. Res. Comm.,* 285, pp 991-996, 2001.

[21] C. Capanni, N. Taddei, S. Gabrieli, L. Messori, P. Orioli, F. Chiti, "Investigation of the effects of copper ions on protein aggregation using a model system", *Cell. Mol. Life Sci.,* 61, pp 982-991, 2004.

[22] S. Rouche, S. Naille, M. Dobenesque, A. Bot, J. C. Jumas, J. L. Cuq, S. Marchesseau, "Iron fortification of skim milk: Minerals and ^{57}Fe Mössbauer study", *Int. Dairy J.,* 19, pp 56-63,. 2009.

[23] F. Gaucheron, "The minerals of milk", *Reprod. Nutr. Dev.,* 45, pp 473-483, 2005.

[24] C. J. Frederickson, "Neurobiology of zinc and zinc-containing neurons", *Int. Rev. Neurobiol.,* 31, pp 145-238, 1989.

[25] J. R. Connor, S. L. Menzies, S. Martin, E. J. Mufson, "A historical study of iron, transferin, and ferritin in Alzheimer's diseased brains", *J. Neurosci. Res.,* 31, pp 75-83, 1992.

[26] R. Aschaffenburg, J. Drewry, "Improved method for the preparation of crystalline b-lactoglobulin and a-lactalbumin from cow's milk", *Biochem. J.,* 65, pp 273–277, 1957.

[27] J. Chakraborty, N. Das, K. P. Das, U. C. Halder, "Loss of structural integrity and hydrophobic ligand binding capacity of acetylated and succinylated bovine β-lactoglobulin", *Int. Dairy J.,* 19, pp 43-49, 2009.

[28] S. Jeyarajah, J. C. Allen, "Calcium binding and salt-induced structural changes of native and preheated β-lactoglobulin", *J. Agric. Food Chem.,* 42, pp 80-85, 1994.

[29] U. K. Laemmli, "Cleage of structural proteins during the assembly of the head of bacteriophage T4", *Nature,* 227, pp 680-685, 1970.

[30] W. Garzon-Rodriguez, A. K. Yatsimirski, C. G. Glabe, "Binding of Zn(II), Cu(II), and Fe(II) ions to Alzheimer's A-beta peptide studied by fluorescence", *Bioorg. Med. Chem. Lett.,* 9, pp 2243-2248, 1999.

[31] G. Verdone, A. Corazza, P. Viglino, F. Pettirossi, S. Giorgetti, P. Mangione, "The solution structure of β2-mirogloulin reveals the problems of its amyloid transition", *Prot. Sci.,* 11, pp 487-499, 2002.

[32] J. Villanueva, M. Hoshino, H. Kardos, K. Hasegawa, H. Naiki, "Increase in conformational flexibility of β_2- micro- globulin upon copper binding: a possible role for copper in dialysis-related amyloidosis", *Prot. Sci.,* 13, pp 797-809, 2004.

[33] M. Hasimoto, L. J. Hsu, Y. Xia, A. Takeda, A. Sisk, M. Sundsmo, "Oxidative stress induces amyloid-like aggregate formation of NACP/synuclein in vitro", *Neuroreport,* 10, pp 717-721, 1999.

[34] C. J. Morgan, M. Gelfand, A. D. Miranker, "Kidney dialysis-associated amyloidosis: a molecular role for copper in fiber formation", *J. Mol. Biol.,* 309, pp 339-345, 2001.

[35] I. S. Lee-Matsui, M. Suzuki, N. Hayasi, J. Hu, L. J. Van-Eldik, K. Titani, M. Nishikimi, "Copper-dependent formation of disulfide-linked dimmer of S100Bprotein", *Arc. Biochem. Biophys.,* 374, pp137-141, 2000.

[36] H. Naiki, K. Higuchi, M. Hosokawa, T. Takeda, "Fluorometric determination of amyloid fibrils in vitro using the fluorescent dye, thioflavin T1", *Anal. Biochem.,* 177, pp 244-249, 1989.

[37] J. R. Lakowich, "Principles of fluorescence spectroscopy", Plenum Press, New York, pp 278-279, 1983.

[38] A. M. Donald, "Aggregation in β-lactoglobulin", *Soft Matt.,* 4, pp 1147-1150, 2008.

[39] Aymard, P., Nicolai, T., Durand, D. "Static and dynamic scattering of β-lactoglobulin aggregates formed after heat-induced denaturation at pH 2", *Macromol.,* 32, pp 2542-2552, 1999.

[40] C. Akkermans, A. J. Van der Goot, P. Venema, E. Van der Linden, R. M. Boom, "Formation of fibrillar whey aggregates: Influence of heat and shear treatment, and resulting rheology", *Food Hydrocoll.,* 22, pp 1315-1325, 2008.

[41] C. Akkermans, A. J. Van der Goot, P. Venema, H. Gruppen, J. M. Vereijken, E. Van der Linden, R. M. Boom, "Micrometer-

sized protein aggregates from soy-glysine and soy protein isolate", *J Agric Food Chem.,* 55, pp 9877-9882, 2007.

[42] J. Seloke, "The molecular pathology of Alzheimer's disease", *Neurones,* 6, 487-498, pp 1991.